Analysis of underwater acoustic data collected under sea ice during the Useful Arctic Knowledge 2021 cruise

William Jenkins, Hayden Johnson, Sofia Vakhutinsky, et al.

Citation: Proc. Mtgs. Acoust. **47**, 070003 (2022); doi: 10.1121/2.0001574
View online: https://doi.org/10.1121/2.0001574
View Table of Contents: https://asa.scitation.org/toc/pma/47/1
Published by the Acoustical Society of America

ARTICLES YOU MAY BE INTERESTED IN

Estimation of uncertainties in underwater sound measurements of ships
Proceedings of Meetings on Acoustics **47**, 070002 (2022); https://doi.org/10.1121/2.0001571

Accuracy of numerically predicted underwater sound of a ship-like structure
Proceedings of Meetings on Acoustics **47**, 070001 (2022); https://doi.org/10.1121/2.0001565

Correlations between sound speed and density in seabed sediment cores collected in Norwegian waters
Proceedings of Meetings on Acoustics **47**, 070004 (2022); https://doi.org/10.1121/2.0001588

Comparison of two different methods to include a beam pattern in parabolic equation models
Proceedings of Meetings on Acoustics **47**, 070006 (2022); https://doi.org/10.1121/2.0001593

Analysis of hydroacoustic time series by parametric predictive modelling
Proceedings of Meetings on Acoustics **47**, 055001 (2022); https://doi.org/10.1121/2.0001596

Sonar array beampattern bounds and an interval arithmetic toolbox
Proceedings of Meetings on Acoustics **47**, 055002 (2022); https://doi.org/10.1121/2.0001613

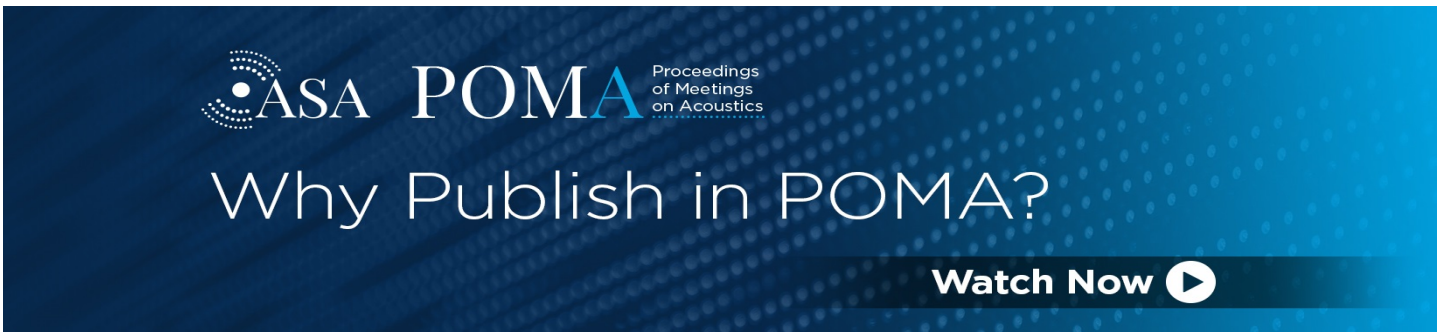

Volume 47 http://acousticalsociety.org/

International Conference on Underwater Acoustics
Southampton, UK
20-23 June 2022
Underwater Acoustics: Polar Acoustics

Analysis of underwater acoustic data collected under sea ice during the Useful Arctic Knowledge 2021 cruise

William Jenkins and Hayden Johnson
Scripps Institution of Oceanography, University of California San Diego, La Jolla, CA, 92093; wjenkins@ucsd.edu; h3johnso@ucsd.edu

Sofia Vakhutinsky and Meghan Nicole Helmberger
University of Colorado Boulder, Boulder, CO, sofia.vakhutinsky@colorado.edu; meghan.helmberger@colorado.edu

Espen Storheim, Hanne Sagen and Stein Sandven
Nansen Environmental and Remote Sensing Center Bergen, Bergen, NORWAY; espen.storheim@nersc.no; hanne.sagen@nersc.no; stein.sandven@nersc.no

Acoustical observations are presented from the Useful Arctic Knowledge (UAK) 2021 cruise, an early-career training program which took place in sea ice north of Fram Strait in June 2021 on board the Norwegian Coast Guard icebreaker KV *Svalbard*. Through oceanographic sampling and three acoustics-related tasks, participants were introduced to practical applications of underwater acoustics and observed the ocean environment and its role in acoustic propagation. Propagation modeling from oceanographic sampling confirmed an upward-refracting environment throughout the cruise. In the first task, a drifting acoustic receiver buoy with a single hydrophone was deployed in an ice floe and left to passively record for eight days. Various biological sounds were recorded, including bearded seals and cetaceans. In the second task, acoustic localization using an active pinger system was used to recover an operational oceanographic mooring from the seabed. The third task involved passive acoustic observations beneath sea ice whenever KV *Svalbard* fastened herself to ice floes and measurements of the ice were made. Through the UAK 2021 cruise, participants learned the utility and value of using underwater acoustics for operations in the Arctic Ocean, particularly in location and retrieval of equipment and in measuring and sensing the environment.

Published by the Acoustical Society of America

© 2022 Acoustical Society of America. https://doi.org/10.1121/2.0001574

1. INTRODUCTION

The Useful Arctic Knowledge (UAK) program is an international, interdisciplinary program hosted by Norway's Nansen Environmental and Remote Sensing Center (NERSC), intended to build and maintain strong partnerships among students, early career scientists, and experienced experts in selected Arctic topics. One of the defining features of the program is an annual scientific cruise. In June 2021, participants from nine countries embarked on board the Norwegian Coast Guard icebreaker KV *Svalbard* and conducted observations of sea ice, acoustic measurements, conductivity-salinity-temperature (CTD) casts, mooring recovery in sea ice, buoy deployments, remote sensing product analysis, and sea ice navigation. This paper presents observations and discussion from tasks related to acoustic observation.

Acoustic and oceanographic observations were made over the course of eight days utilizing CTD casts and passive and active acoustics. On 8 June, a drifting acoustic receiver buoy with several instruments was deployed in an ice floe and left to passively record for eight days. An acoustic localization of the buoy was demonstrated before the *Svalbard* continued on with her cruise. At various points in the subsequent week, *Svalbard* fastened herself to ice floes where measurements of the ice were made. At each of these ice stations, passive acoustic observations were made. On 12 June, acoustic localization was used to successfully estimate the position of an oceanographic mooring for recovery. On 16 June, the *Svalbard* located and recovered the drifting acoustic receiver buoy.

The purpose of the acoustic tasks was to introduce participants to practical applications of underwater acoustics, including equipment selection and preparation, mooring construction, deck handling, and collection and handling of data. Furthermore, participants observed the ocean environment and its role in underwater acoustic propagation. Finally, participants learned the utility and value of using underwater acoustics for operations in the Arctic Ocean, particularly in location and retrieval of equipment and in measuring the environment. In the sections that follow, a description of the acoustic environment is provided, and each acoustic task is discussed in detail.

2. ENVIRONMENT

A. ENVIRONMENTAL SAMPLING

The Arctic Ocean is generally an upward refracting environment.[1] Unlike more temperate latitudes where water at the surface is warmer than at depth, surface waters in the Arctic are typically cooler and fresher, resulting in lower sound speeds, although intrusion of warmer, more saline water does occur at inflows in the Fram Strait and Bering Strait.[2,3] In Fram Strait, a great deal of oceanographic variability occurs due to Atlantic Water transported by the West Spitsbergen Current,[2] which has been measured directly with oceanographic measurements[4] and acoustically in various tomography experiments.[5,6] In the Arctic, the ambient noise field is related to transients generated by sea ice as well as biological activity and anthropogenic sources such as seismic airgun surveys.[7]

As part of an ongoing series of oceanographic measurements in Fram Strait and north of Svalbard, eight CTD casts were performed at various points throughout the cruise. Figure 1a shows sampling locations and results for each CTD cast. Casts 1 through 7 show typical sound speed profiles (SSP) for the Arctic Ocean, with the top 100 m strongly influenced by relatively cold, fresh water. In cast 8, the strength of the layer is substantially diminished, likely as a result of Atlantic Water intrusion through Fram Strait.

Additional CTD data were collected using expendable bathythermographs (XBT) and were consistent with profiles shown in Fig. 1a, and a continuously recording CTD instrument was mounted to the drifting acoustic receiver buoy (Sec. 3).

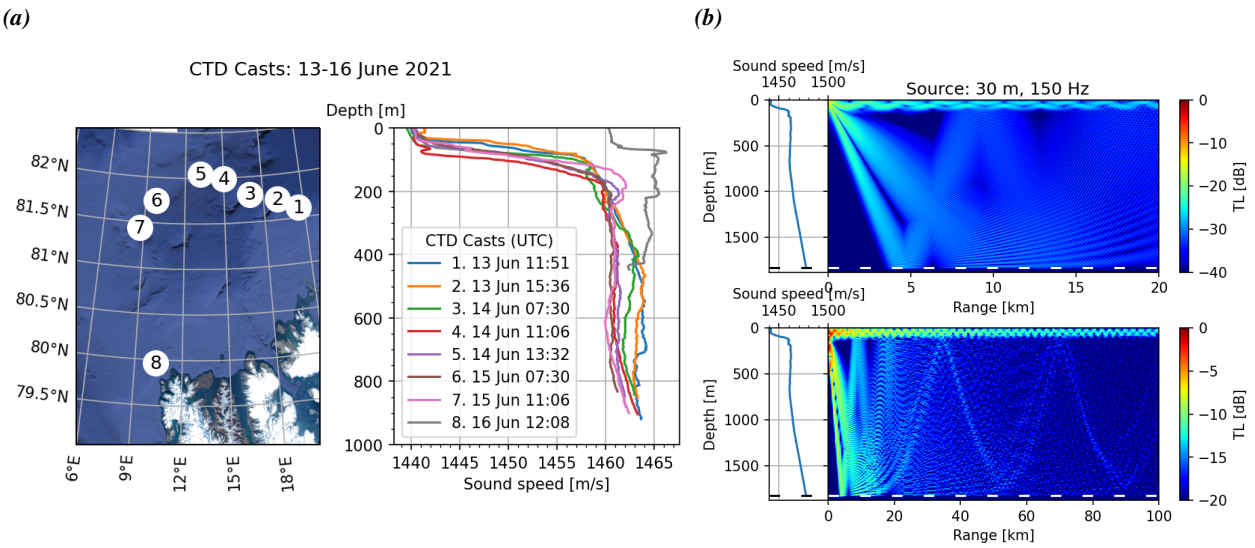

Figure 1: (a) Conductivity/temperature/depth (CTD) instrument casts taken throughout the cruise. (b) Transmission loss for a source at 10.5 m, 200 Hz using KRAKEN normal mode propagation model for 20 km (top) and 100 km (bottom). The sound speed profile used for the model is shown in the left panels and is from an XBT shot during the acoustic localization training described in Sec. 4.

B. ACOUSTIC PROPAGATION MODELING

CTD profiles revealed an upward refracting environment which led to a surface duct in the upper sonic layer. A combination of relatively fresh water combined with water cooled by the Arctic air results in especially slow sound speeds in the upper ocean. Figure 1b shows a simplified acoustic propagation model for transmission loss (TL) using environmental data collected by an XBT during an acoustic localization exercise (Sec. 4). The KRAKEN normal mode propagation model[8] was used to compute transmission loss for a 150 Hz source positioned at a depth of 30 m, which is the approximate depth of the hydrophone on the receiver buoy (Sec. 3). TL is shown out to a range of 20 km (Fig. 1b, upper panel) and 100 km (Fig. 1b, lower panel). Surface ducting is visible in both panels, with the sonic layer depth located at the thermocline at a depth of approximately 150 m. The SSP below the thermocline was also positive, and in the lower panel of Fig. 1b there is a half channel with annuli occuring approximately every 35 km. A 2 m layer of ice is assumed, but this modeling does not take into account ice roughness, thus TL is underestimated as ice scatters and reflects sound into the ocean bottom. Nevertheless, the model shows that the dominant propagation paths are direct path (close range), surface duct (medium range due to the frequent interactions with the ice and surface scattering), and half-channel surface bounce, especially for smaller launch angles in deeper water.

3. DRIFTING ACOUSTIC RECEIVER BUOY

A. EQUIPMENT, DEPLOYMENT, AND RECOVERY

The drifting acoustic receiver buoy consisted of a weighted line approximately 35 m long suspended from a float. A Multi-électronique µAURAL recorder with an integrated HTI 96-min hydrophone, sampling continuously at 48 kHz sampling frequency, was mounted on the line at 30 m depth. A Sea-Bird Scientific SBE37 CTD, sampling with an interval of five minutes, was mounted at 33 m depth. A XEOS GPS receiver was fastened to the float itself, and recorded the position of the float every hour. An Edgetech Coastal Acoustic Transponder (CAT) was mounted for acoustic localization.

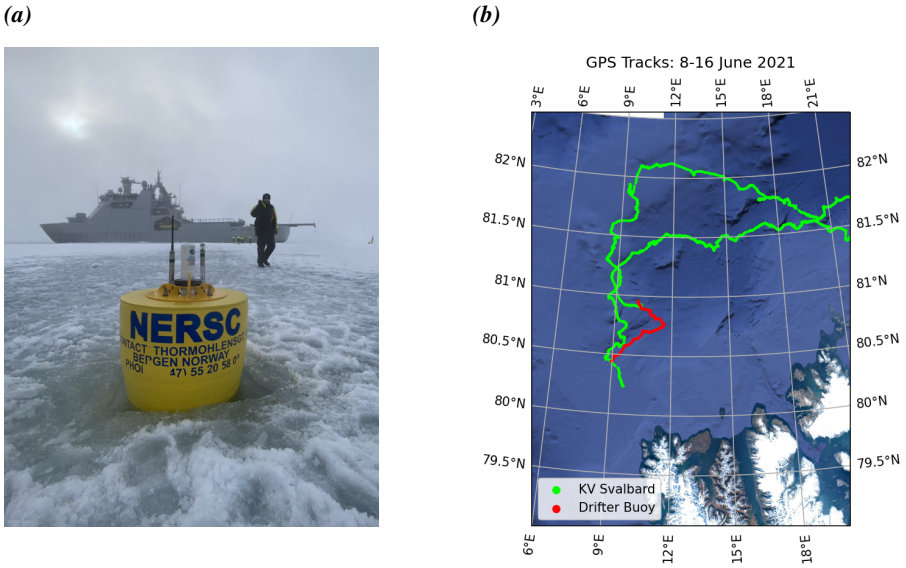

Figure 2: (a) Deployment of the drifting acoustic receiver buoy on an ice floe. (Photo: William Jenkins) (b) The track of KV* Svalbard *(green) and the buoy (red) are shown for the duration of the buoy deployment.

The buoy was deployed on 8 June 2021 at 17:52 CET in an ice floe located at $80°57.855'\mathrm{N}$ and $010°09.437'\mathrm{E}$. To ensure the buoy remained fixed to the ice floe, a hole was drilled through the ice large enough for the instruments to pass through, but small enough that the float would remain lodged at the surface. In the event the ice floe were to melt or fail, the float ensured the instruments would not sink. The buoy deployment is depicted in Fig. 2a.

The drifting buoy and hydrophone were retrieved from the ice floe on 16 June 2021 at 09:09 CET at $80°26.045'\mathrm{N}$ and $008°59.338'\mathrm{E}$. The buoy's GPS transceiver provided general localization, and as the *Svalbard* approached, the buoy was identified visually. The buoy had cumulatively traveled 108.7 km, and as seen in Fig. 2b, initially drifted southeast, then changed directions to the southwest.

B. DATA ANALYSIS

The ice floe that the drifting acoustic receiver buoy was fastened to thinned over the course of the deployment, with a measured ice thickness of about 70 cm at the start of the deployment and about 30 cm upon recovery. Previous studies suggest melting sea ice produces sound underwater in the frequency range of a few hundred Hz to a few kHz.[9] To assess whether this signal is observable in our data, we compare the sound power measured by the hydrophone in several frequency bands to measured or modeled (ERA5 reanalysis[10]) environmental variables which could reasonably be expected to be indicative of melting of the sea ice near the buoy.

It is apparent visually from Fig. 3, and from the correlations presented in Table 1, that the dominant feature in the integrated sound power is an increase in the energy present at low frequencies corresponding to times when the over-ground speed of the buoy and the ERA5 10 m wind speed. By listening to the recordings, it was determined that most of this energy is likely a result of strum noise due to the motion of the buoy through the water. The depth of the CTD, computed from the measured pressure, can be seen to decrease at the periods with the highest speed over ground, suggesting that there was sufficient force being exerted on the cable and instrumentation to cause the line to tilt away from vertical, which adds support for the hypothesis of strum noise. It seems likely that the correlation between wind speed and sound power at low frequencies is at least partially a result of the causal relationship between wind speed and the speed of

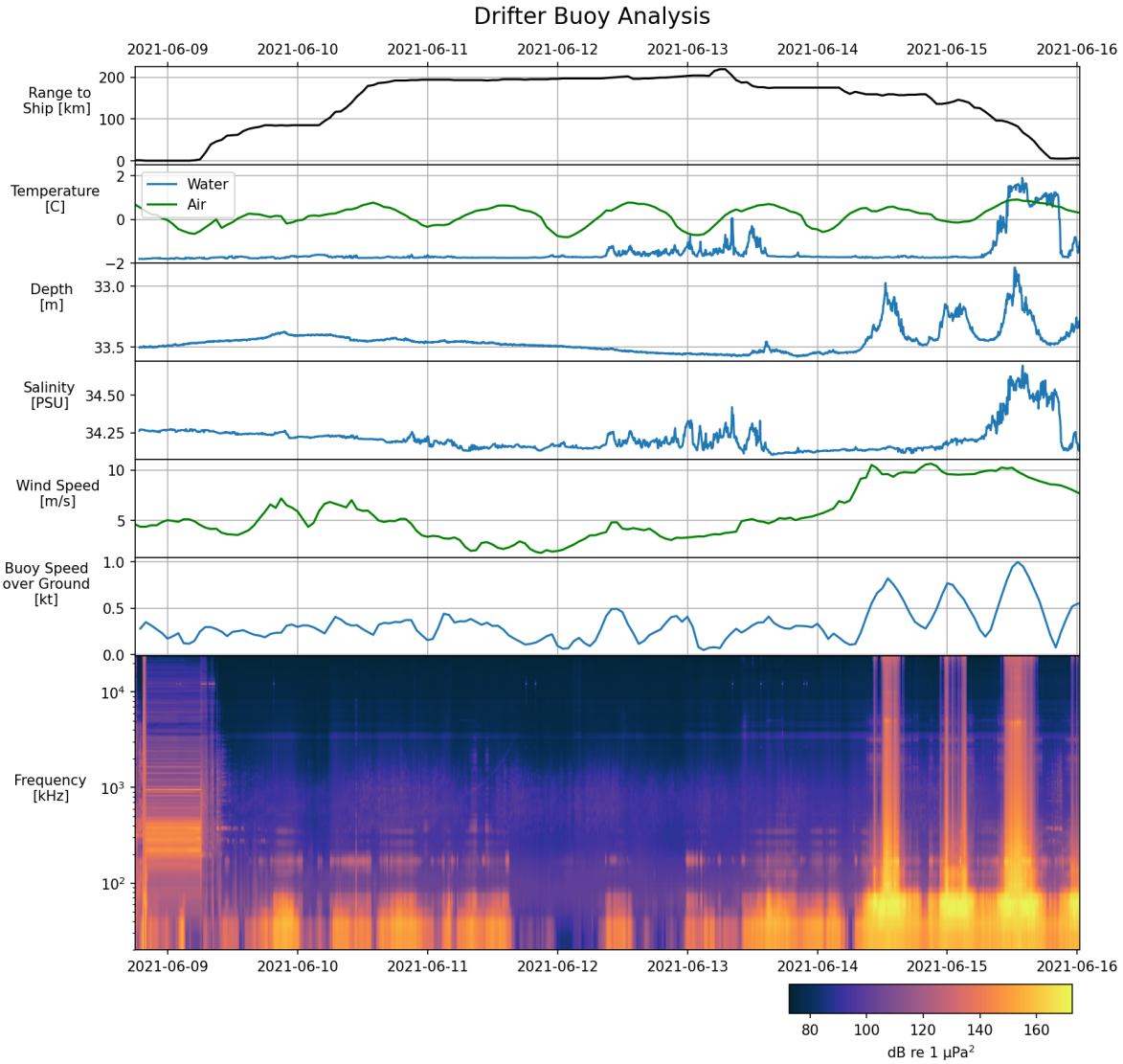

Figure 3: Time series of various environmental variables, which were measured on the drifting acoustic receiver buoy by the CTD (water temperature, salinity), GPS (buoy speed over ground, range to ship), or taken from ERA5 reanalysis products (air temperature, wind speed). The bottom panel is a spectrogram of the acoustic data recorded by the hydrophone over the duration of the deployment, showing the distribution of energy over frequencies. Note that the sharp vertically uniform bands of high energy are periods where the sound was sufficiently loud to saturate the recording; these periods have accordingly been removed from the analysis presented in Table 1.

the ice flows, which determines the speed of the buoy. However, the weak but still elevated correlations between wind speed and sound power even at high frequencies, where buoy speed over ground and sound power are completely uncorrelated, suggests that wind acting on the available area of open water could be causing some increase in underwater noise.

Even outside the low-frequency band dominated by the strum noise, we find no clear relationship between the environmental variables that might be indicative of melting and the sound power in any frequency band. The slight rise in water temperature during the middle of the record does not correspond to any discernible increase in sound power, and the rise in water temperature near the end of the record unfortunately corresponds with a period of hydrophone saturation.

Table 1: Correlation between various environmental factors and the logarithm of sound power integrated over different frequency bands.

	Frequency (kHz)				
Parameter	0-0.3	0.3-1	1-3	3-10	10-24
Water temperature	0.1004	0.0662	0.0943	0.1351	-0.0093
Buoy speed over ground	0.4707	-0.0241	0.0603	0.0828	-0.0950
ERA5 10 m wind speed	0.6358	0.1232	0.2302	0.3216	0.0169
ERA5 2 m air temperature	0.2349	-0.0900	-0.0452	-0.0272	-0.1085

C. HIGHLIGHTS

In this section, we highlight several signals recorded by the drifting acoustic receiver buoy that were representative of the broader soundscape observed during the recording period. The biologic examples that follow were excerpted from the morning of 12 June, when the record had the lowest ambient and self noise. During this quiet period, many types of marine mammals and fish vocalizations could be heard. The Discovery of Sound in the Sea website[11] was used to identify animals based on vocalization characteristics; however, the audio examples on the website are somewhat limited, and it was not possible to positively identify all of the vocalizations.

Though the data from the morning of 12 June can be readily analyzed for biologic sources, it is noteworthy that, in spite of the noise of the strumming buoy wire, biologic sources were detected throughout the entirety of the record. The most prominent and easily identifiable sources were bearded seals. Cetaceans were also heard throughout the record and were most likely narwhals or beluga whales. Throughout the record, broadband pops and clicks were observed, some of which were likely associated with echolocation from marine mammals, although species attribution based on a single impulse was not possible. In addition to biologic sources, anthropogenic sounds such as machinery, propulsion, and icebreaking from the *Svalbard* are heard in the first two days of the record.

i. KV *Svalbard* self-noise

After deploying the buoy, KV *Svalbard* continued to drift with the ice floe overnight with her propulsion secured. Of course, various hotel loads and machinery continued operating. In recordings made near the *Svalbard*, including those from later ice stations, a periodic clicking noise was heard and is shown in the spectrogram in Fig. 4a, with a stronger click followed by a weaker click. The period of the full cycle was 1.75 s. Owing to the regular periodicity of this signal, it is likely generated by a rotating piece of machinery operating at approximately 34.3 RPM.

KV *Svalbard* was underway again on the morning of 9 June to conduct acoustic ranging to the buoy. Fig. 4b shows a spectrogram of the *Svalbard* maneuvering through sea ice. Below 1.5 kHz the propulsion machinery dominates the spectrum. Above 1.5 kHz, the spectrum becomes saturated with broadband noise as the ship impinges on ice and breaks it apart. Periods when the ship was in open water are indicated by regions of low energy above 1.5 kHz.

ii. Bearded seals

Bearded seals were heard constantly throughout the entire record. These seals emit a warbling sound that sweeps downward in frequency, with occasional upshifts. From Fig. 4c, the duration of some of these

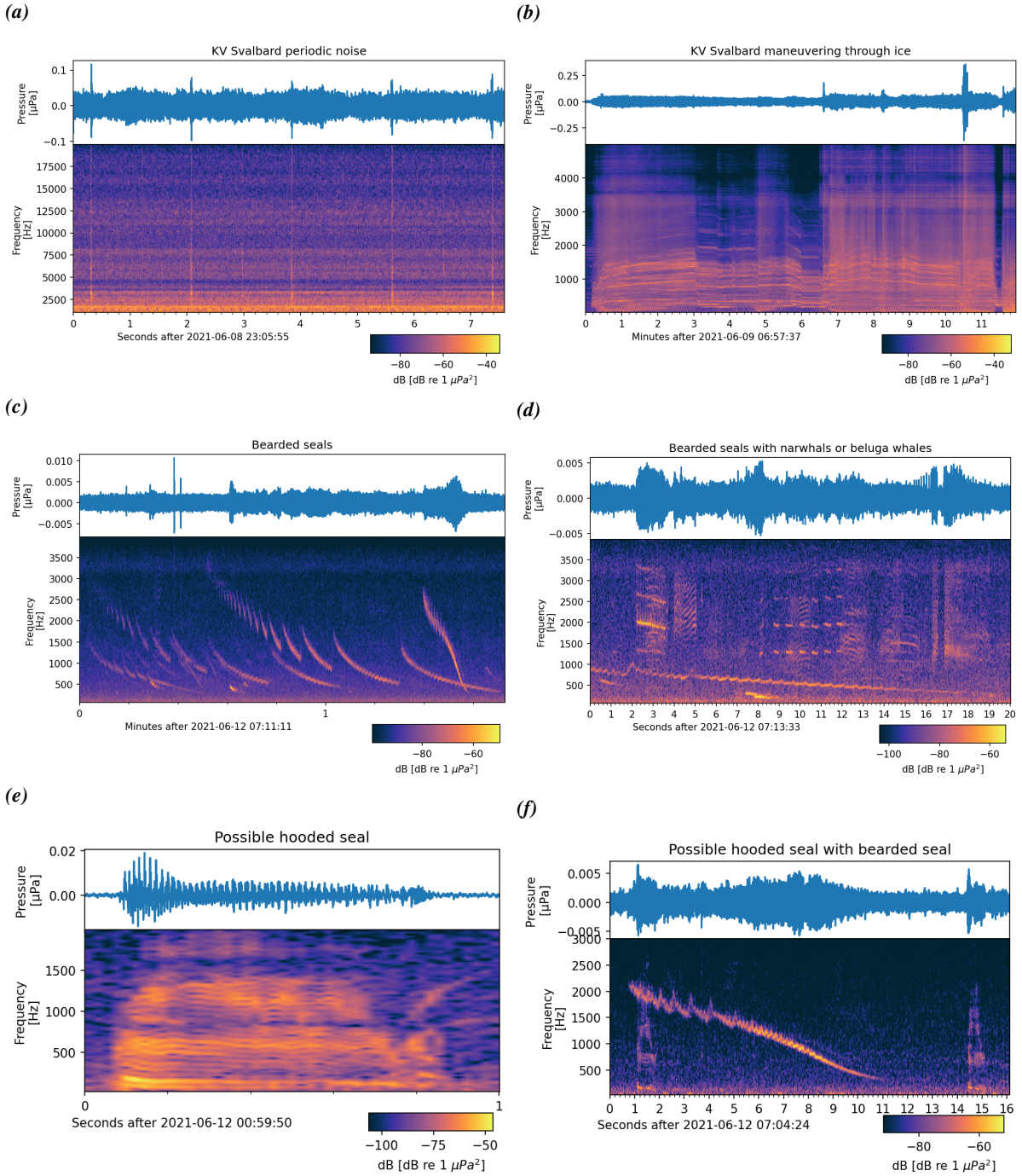

Figure 4: *(a) Periodic transients from KV* **Svalbard** *suggest rotating machinery as the source. (b) KV* **Svalbard** *maneuvering through sea ice. (c) Bearded seal vocalizations. (d) Marine mammal vocalizations, including a downsweep made by a bearded seal (below 1 kHz) and vocalizations from narwhals or beluga whales. (e) Possible hooded seal vocalization. (f) Possible hooded seal vocalizations appear at the beginning and end of the spectrogram, shown with an intervening bearded seal call.*

calls was greater than one minute. As June was in the middle of their mating season, these calls may be attempts to attract mates. Bearded seals were spotted from the *Svalbard* on sea ice throughout the cruise.

iii. Narwhals or beluga whales

Figure 4d shows examples of vocalizations from several biologic sources. The long, warbling downsweep of a bearded seal is visible below 1 kHz over the course of the entire spectrogram. Fine striations above 1 kHz sweeping rapidly up and down are likely narwhals or beluga whales, and were heard throughout the entire record. A vocalization with fundamental frequency at approximately 1.3 kHz and harmonics at 700 Hz intervals is observed with a single call at 2 s, followed by a repetitive train of pulses between 8 and 12 s; this, too, was likely a a narwhal or beluga.

iv. Possible hooded seals

One of the biologic sources was recorded on numerous occasions between 10-13 June appears to be a call from a hooded seal. These animals would emit single vocalizations as well as call repeatedly two to three times per minute for several minutes. The vocalization sounds like a deep, nasal "wow," with the beginning of the signal shifting downward in frequency, and at the very end sweeping up. Figure 4e shows the vocalization in detail, and Fig. 4f shows its co-occurrence with a bearded seal vocalization. While hooded seals are typically asocial, June marks the end of their mating season and these calls may be indicative of animals seeking a mate.[12]

4. ACOUSTIC LOCALIZATION OF MOORINGS

One of the primary acoustic tasks was to localize an oceanographic mooring for recovery. This is an especially challenging activity in the Arctic that requires careful coordination between the ship's bridge, deck hands, and acoustic operators. First, a patch of sea ice must be cleared over the mooring. This can be done by icebreaking or waiting for a lead to pass over the mooring. Second, the ship must triangulate the position of the mooring using acoustic two-way travel times. Finally, once the mooring is localized, an acoustic release activates and the mooring floats to the surface for recovery. The entire procedure must occur as swiftly as possible since the sea ice is moving with the wind and current. Thus, the validity of the localization quickly becomes invalid, and the mooring could come up beneath the sea ice when released.

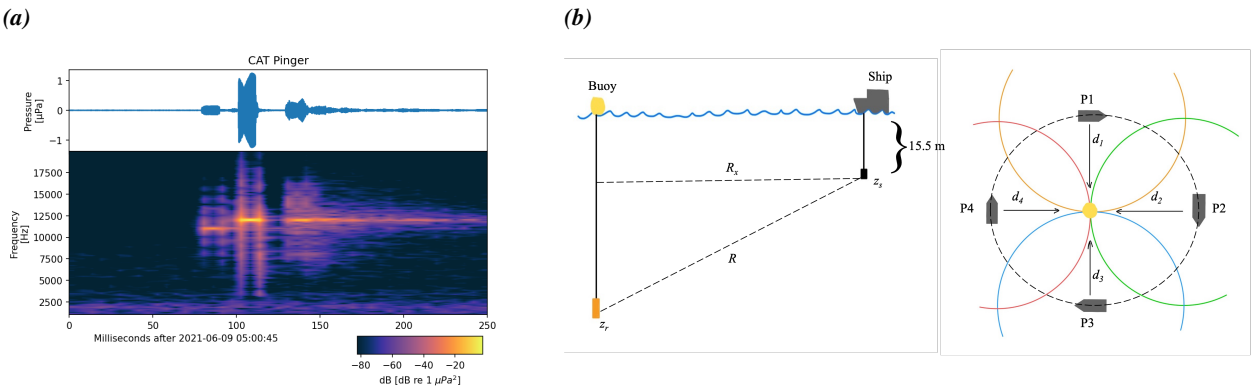

Figure 5: (a) Acoustic localization signals. The 11 kHz tone was transmitted by KV Svalbard, and the 12 kHz tone was the response transmitted by the transducer on the drifting acoustic receiver buoy. (b) Active acoustic localization betwen a ship and a buoy. R_x is used to plot range rings around the ship's position, and the buoy is localized at the intersection of multiple range rings.

A. EQUIPMENT

An Edgetech CAT pinger worked in tandem with a shipboard transducer to perform active acoustic localization. On board KV *Svalbard*, a deck unit drove a transducer that produced an 11 kHz outbound signal. The CAT, upon receiving the 11 kHz signal, transmitted a 12 kHz signal. On board *Svalbard*, the time elapsed between the transmission of the 11 kHz signal and receipt of the 12 kHz signal constituted the two-way travel time. Assuming an average speed of sound in water, the distance between the source and receiver could be estimated. In Fig. 5a, a spectrogram of the sequence of localization signals is shown.

B. METHODOLOGY

Two-way travel times Δt were measured as the time T elapsed between the transmission of the 11 kHz signal and reception of the 12 kHz signal, plus a correction T^* to account for the delay on board the CAT pinger betwen its reception of the 11 kHz signal and transmission of the 12 kHz signal. The one-way travel time is then:

$$\Delta t = \frac{T}{2} - T^*. \tag{1}$$

Slant range R between the ship and the CAT pinger is then:

$$R = c_{\text{avg}} \Delta t, \tag{2}$$

where c_{avg} is the average sound speed between the two. Finally, the horizontal range R_x is given by:

$$R_x = \sqrt{R^2 - |z_r - z_s|^2}, \tag{3}$$

where z_r and z_s are the depths of the CAT pinger and ship's transducer, respectively.

Since the ship's transducer is a single, omnidirectional element, it is impossible to resolve bearing to the CAT pinger with a single measurement. To localize the buoy, several measurements are taken at different positions, with circles of radius R_x plotted at each position of measurement. Where the circles intersect indicates the estimated position of the mooring.[13] A schematic of the localization procedure is shown in Fig. 5b.

C. RESULTS

i. Practice localization on known position

Acoustic localization was tested on the drifting acoustic receiver buoy on 9 June 2021. With a GPS receiver mounted on top of the buoy, the localization results could be compared to the actual positions of the buoy and ship. Two localizations were performed at ranges of approximately 500 m and 1000 m. For each localization, four measurements were taken at approximately 90° intervals around the buoy.

At each measurement position, the shipboard acoustic transducer was lowered to $z_s = 15.5$ m below the surface of the water. A piece of tape was attached to the wire marking how far the source needed to be lowered so that the depth would be consistent between measurements. After the transponder was lowered to the correct depth, the position of the ship was recorded and the 11 kHz signal was transmitted. Once the 12 kHz signal from the CAT arrived at the ship, the two-way travel time T was recorded and a time delay $T^* = 12.5$ ms used to obtain Δt. From XBT casts performed in the area, average SSP was $c_{avg} = 1442$ m/s. Using the CAT pinger depth of $z_r = 33$ m, horizontal range was calculated at each measurement position using Eq. 1–3. Table 2 includes an example of data collected during the localization.

At this point, participants were divided into two groups to estimate the position of the buoy for the 500 m localization and 1000 m localization. Using the horizontal ranges, each group plotted its range

Table 2: Example of two-way travel time data collected during acoustic localization.

	Ship Position			
Time	Latitude	Longitude	T (ms)	R_x (m)
05:02	80°55.3501'N	010°13.9118'E	851	627
05:15	80°55.1844'N	010°16.5782'E	656	478
05:35	80°55.4784'N	010°18.3356'E	865	636
05:53	80°55.5761'N	010°16.4029'E	795	589

circles, but exact intersections were not obtained due to measurement errors and other factors. The most significant of these was that, because of the wind and currents, the ship and buoy were moving at slightly different velocities which were not accounted for in the calculations. Despite these errors, the experiment still produced areas of intersection where the buoy had the highest probability of being located. The two groups then independently developed ways to account for these errors and the effect of time elapsed between measurements, incorporating a linear rate of ice drift to estimate the buoy's position. KV *Svalbard*'s track, both buoy localization estimates, and the hourly GPS positions reported by the buoy are shown in Fig. 6. For the 500 m localization, there was an estimated error of 70.3 m, while for the 1000 m localization there was an estimated error of 81.5 m. Since during recovery operations cleared sea ice typically spans several hundred meters, these errors were within the tolerance for successfully recovering a mooring.

ii. Recovery of an oceanographic mooring

On the afternoon of 11 June 2021, KV *Svalbard* took station over oceanographic mooring CNRS23, which was deployed in 2019 to observe Atlantic Water inflow into the Arctic Ocean.[14] Recovery was timed to coincide with the occurrence of a large lead of open water over the mooring. While the position of the mooring was known from its 2019 deployment, acoustic localization was performed to confirm its location prior to recovery. Once the location was confirmed, an acoustic release was activated and the mooring

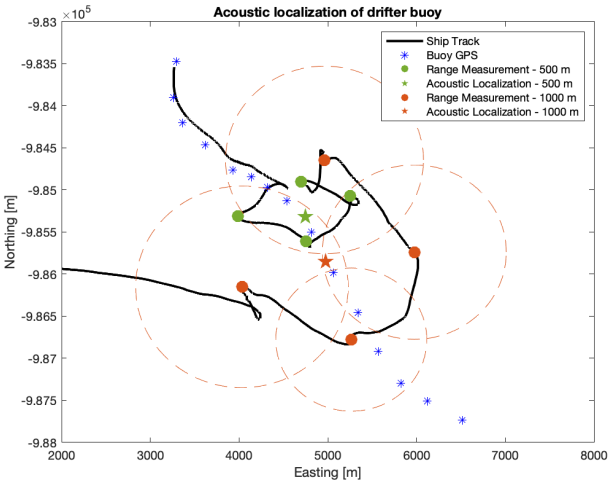

Figure 6: Results are shown from acoustic localizations conducted at a range of 500 m and 1000 m. Drifter buoy GPS positions are hourly.

Figure 7: Oceanographic mooring CNRS23, shown here being recovered by KV* Svalbard*, was localized using active acoustics before being released from its anchor. (Photo: Sofia Vakhutinsky)

floated to the surface. A small boat was deployed to retrieve the mooring, and the mooring with its numerous oceanographic instruments was recovered with the ship's crane as shown in Fig. 7.

5. ICE STATIONS

Additional acoustic measurements were taken with a hydrophone lowered by hand through a hole drilled in the sea ice during sea ice station measurements. Most of the time, mechanical noise from the nearby ship was far louder than any environmental signals that might have been of interest. One exception is the controlled explosion, described here.

On the evening of 14 June, KV *Svalbard* stationed herself on an ice floe located at $82°05.607'\mathrm{N}$ and $010°02.179'\mathrm{E}$. Though the main purpose of this visit was to observe ice ridges on the floe, an interesting opportunity for acoustic measurement arose when the ship's crew was given permission to detonate expired explosives. Using one of the many holes drilled for ice ridge observation, a hydrophone was lowered beneath the ice to capture the explosion as heard underwater. The explosives were emplaced in the ice approximately two hundred meters away.

Explosions create an impulsive signal, enabling an estimate of the bottom depth using acoustic travel times. The distance traveled by an acoustic wave is $d = ct$, where c is the speed of sound and t is the time elapsed. In this case, since the acoustic signal is traveling to the bottom of the ocean and back, t is the two-way travel time and must be divided by two to give the bottom depth z_b:

$$z_b = \frac{ct}{2} \tag{4}$$

Because the depth of the ocean is much greater than the distance between the source and receiver at the surface, the source and receiver are assumed to be in the same position. Figure 8 shows the normalized acoustic pressure and spectrogram of the recorded signal. The two-way travel time is obtained from the time difference of arrival between the first and second impulses. Using an estimated average sound speed of 1490 m/s and a measured time difference of arrival of 1.293 s, the bottom depth is estimated to be 963 m at this location, which is consistent with bathymetric data from the International Hydrographic Organization.

Figure 8 contains some noteworthy propagation features. The first wave packet appears to contain multiple sub-packets of energy. This is likely a combination of two factors. First, several explosives were

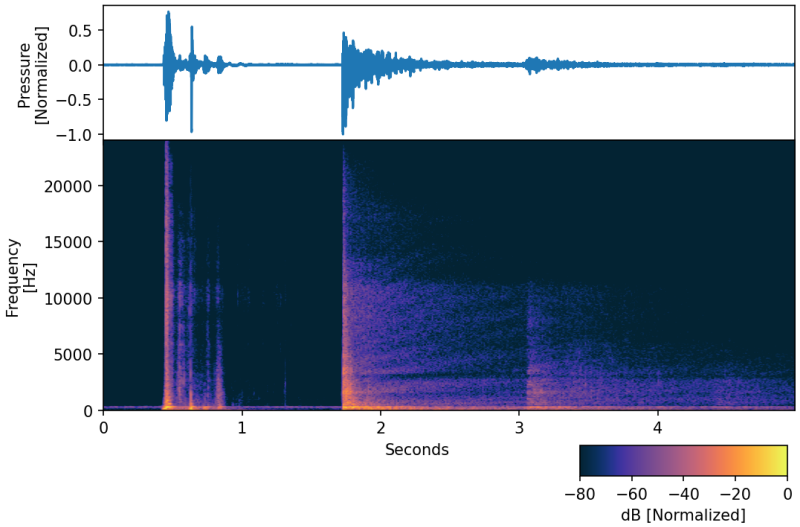

Figure 8: Normalized time series and spectrogram of explosives detonation on sea ice, followed by first and subsequent bottom bounce reflections.

detonated, but due to latency in the detonation cord and fuses, they did not detonate simultaneously. The asynchronous detonation was recorded on film and audio by the observers. Second, because the explosives were emplaced within the ice, energy propagates seismo-acoustically through elastic media (the ice) as well as through the water. The speed of propagation for longitudinal waves in ice is approximately 3,800 m/s, and shear waves are approximately 1,800 m/s.[15] As these waves propagate outward through the ice, energy along this wavefront is transmitted into the water. These elastic modes of propagation are likely the first arrivals recorded, followed by direct path propagation through water between the source and the receiver. Since the ocean acts as an acoustic waveguide, the second packet of energy exhibits geometric dispersion, with an interference pattern taking shape as bands of energy through time and frequency following the arrival of the impulse. A third, weaker arrival remains impulsive, but is further attenuated and dispersed than the second arrival.

6. CONCLUSION

The 2021 UAK cruise successfully demonstrated the use of both active and passive underwater acoustics for observation and localization in a challenging and dynamic sea ice environment. Additionally, oceanographic and atmospheric observations were used to model the acoustic propagation environment and to explain observations. Participants received hands-on experience at nearly every stage of the various acoustic tasks, and gained solid insights into the utility of underwater acoustics as both a practical tool for handling oceanographic equipment, as well as a method for observing the environment.

ACKNOWLEDGEMENTS

Mapping data provided by Google Earth. This work was made possible by: Integrated Arctic Observing System (INTAROS) Project H2020 (EU CORDIS grant no. 727890); Research Council of Norway (contract no. 274891); and Office of Naval Research (ONR) Global. The authors would like to thank the officers and crew of KV *Svalbard* for their highly professional support of this cruise. Participants were additionally instructed by Agnieszka Beszczynska-Möller (Institute of Oceanology, Polish Academy of Science), Alistair Everett (Norwegian Meteorological Institute), Tom Rune Lauknes (Norwegian Research Centre AS), and Elena McCarthy (ONR Global). Additional participants included Astrid Stallemo (NERSC); Anna Mathea Skaar, Mads Skjerven Moldrheim, Güney Dinçtürk, and Elinor Tessin (University of Bergen); and Anna Telegina, Laust Færch, and Jozef Rusin (University of Tromsø).

REFERENCES

[1] Robert J. Urick. *Principles of Underwater Sound*. Peninsula Publishing, 1983.

[2] Lynne D. Talley, George L. Pickard, William J. Emery, and James H. Swift. *Descriptive Physical Oceanography: An Introduction*. Academic Press, 2011.

[3] Peter F. Worcester and Megan S. Ballard. Ocean acoustics in the changing Arctic. *Physics Today*, 73(12):44–49, December 2020.

[4] M. Dolores Pérez-Hernández, Robert S. Pickart, Daniel J. Torres, Frank Bahr, Arild Sundfjord, Randi Ingvaldsen, Angelika H. H. Renner, Agnieska Beszczynska-Möller, Wilken-Jon Appen, and Vladimir Pavlov. Structure, Transport, and Seasonality of the Atlantic Water Boundary Current North of Svalbard: Results From a Yearlong Mooring Array. *Journal of Geophysical Research: Oceans*, 124(3):1679–1698, March 2019.

[5] Hanne Sagen, Brian D. Dushaw, Emmanuel K. Skarsoulis, Dany Dumont, Matthew A. Dzieciuch, and Agnieszka Beszczynska-Möller. Time series of temperature in Fram Strait determined from the 2008–2009 DAMOCLES acoustic tomography measurements and an ocean model. *Journal of Geophysical Research: Oceans*, 121(7):4601–4617, July 2016.

[6] Hanne Sagen, Peter F. Worcester, Matthew A. Dzieciuch, Florian Geyer, Stein Sandven, Mohamed Babiker, Agnieszka Beszczynska-Möller, Brian D. Dushaw, and Bruce Cornuelle. Resolution, identification, and stability of broadband acoustic arrivals in Fram Strait. *The Journal of the Acoustical Society of America*, 141(3):2055–2068, March 2017.

[7] Emma Ozanich, Peter Gerstoft, Peter F. Worcester, Matthew A. Dzieciuch, and Aaron Thode. Eastern Arctic ambient noise on a drifting vertical array. *The Journal of the Acoustical Society of America*, 142(4):1997–2006, October 2017.

[8] Michael B. Porter. The KRAKEN normal mode program. *SACLANT Undersea Research Centre Memorandum (SM-245)/Naval Research Laboratory Memorandum Report 6920*, September 1991.

[9] Madan M. Mahanty, G. Latha, R. Venkatesan, M. Ravichandran, M. A. Atmanand, A. Thirunavukarasu, and G. Raguraman. Underwater sound to probe sea ice melting in the Arctic during winter. *Scientific Reports*, 10(1):16047, December 2020.

[10] Hersbach, H., Bell, B., Berrisford, P., Biavati, G., Horányi, A., Muñoz Sabater, J., Nicolas, J., Peubey, C., Radu, R., Rozum, I., Schepers, D., Simmons, A., Soci, C., Dee, D., and Thépaut, J-N. ERA5 hourly data on single levels from 1979 to present, 2018.

[11] University of Rhode Island and Inner Space Center. Audio Gallery. https://dosits.org/galleries/audio-gallery/, June 2017.

[12] NOAA Fisheries. Hooded Seal. https://www.fisheries.noaa.gov/species/hooded-seal, Wed, 03/23/2022 - 15:25.

[13] U. Send, M. Visbeck, and G. Krahmann. Aspects of acoustic transponder surveys and acoustic navigation. In *'Challenges of Our Changing Global Environment'. Conference Proceedings. OCEANS '95 MTS/IEEE*, volume 3, pages 1631–1642 vol.3, 1995.

[14] Centre national de la recherche scientifique. CNRS mooring observations at 22°E 81°28'N in the Atlantic Water inflow north of Svalbard - INTAROS Data Catalogue. https://catalog-intaros.nersc.no/dataset/cnrs-mooring-observations-at-22-e-81-28-n-in-the-atlantic-water-inflow-north-of-svalbard, March 2022.

[15] Christian Vogt, Karim Laihem, and Christopher Wiebusch. Speed of sound in bubble-free ice. *The Journal of the Acoustical Society of America*, 124(6):3613–3618, December 2008.